Journal of Sound and Vibration (1999) **223**(3), 467–482
Article No. jsvi.1999.2155, available online at http://www.idealibrary.com on IDEAL®

TRANSVERSE VIBRATIONS OF A FLEXIBLE BEAM SLIDING THROUGH A PRISMATIC JOINT

M. GÜRGÖZE

Faculty of Mechanical Engineering, *İstanbul Technical University*, 80191 *Gümüşşuyu*, *Istanbul*, *Turkey*

AND

S. YÜKSEL

Department of Mechanical Engineering, *Faculty of Engineering and Architecture*, *Gazi University*, 06570 *Maltepe*, *Ankara*, *Turkey*

(*Received* 16 *November* 1994, *and in final form* 5 *January* 1999)

In this paper, the vibrations of an axially moving flexible beam sliding through an arbitrarily driven prismatic joint, restricted to move on a horizontal plane, are investigated. Upon considering the assumption of an Euler–Bernoulli beam in addition to the effects of rotary inertia, end-mass and axial force in association with axial foreshortening, the equations of motion and the associated boundary conditions of the dynamic system are derived by using the extended Hamilton's principle, forming a complex boundary value problem. Due to difficulties in finding an analytical solution, the assumed modes method is utilized to obtain an approximate solution to the problem. Simulation results are presented for some typical kinematical inputs of the prismatic joint of the model.

1. INTRODUCTION

Having many applications in manipulators and spacecraft appendages, axially moving flexible beams have received considerable attention lately. As one of the earliest works on this subject, Tabarrok *et al*. [1] studied a clamped–free beam whose length varies with time. They considered the beam in flexure, derived the equations of motion using Newton's law and presented certain properties of the mode shapes. In the following studies reported in the literature, some researchers have searched for direct analytical solutions for this vibration problem, like Bergamaschi and Sinopoli [2], while most of them have used approximate methods [3–27].

Considering the eigenfunctions of a clamped–free beam as trial functions of the desired series solution, Wang and Wei [3] and Tadikonda and Baruh [4] have derived the equations of motion, a system of second order ordinary differential equations, for a clamped–free beam whose length varies, and they

0022–460X/99/230467 + 16 $30.00/0

presented some sample results. Similarly, Buffinton and Kane [5] used Kane's method and assumed modes method by taking the eigenfunctions of the clamped–free beam in flexure to investigate the dynamics of a free–free beam moving over supports. Furthermore, Lee [6] formulated the equations of motion in matrix form for a finite beam moving over supports by making use of Hamilton's principle and assumed modes method. He has investigated the response of a beam undergoing various prescribed motions. A recent study on this type of axially moving beam has been due to Stylianou and Tabarrok [7, 8]. They first developed a finite element formulation with time varying domains and illustrated its use through time integration of equations of motion for axially moving beams [7]; later, they examined the stability characteristic of the problem [8]. On the other hand, Theodore *et al.* [9] presented a discussion about the applicability of using separation of variables for discretizing a translating flexible beam with an end mass. In their study, based on the concept of group velocity of the dispersive waves in beam, a non-dimensionalized Euler–Bernoulli beam equation was derived. As the most recent work on this subject, Al-Bedoor and Khulief [10] introduced a systematic approach to obtain an approximate analytical solution for the vibrational motion of a beam with different end conditions, during axial deployment at constant velocity.

On the other hand, an axially moving beam having rotational motion in addition to translational motion was studied by Yuh and Young [11] and Banerjee and Kane [12]. In reference [11], they formulated the problem via Newton's law and Galerkin's discretization method, whereas in reference [12], a new modelling method has been proposed for the simulation of the motion of any continua that undergoes extrusion from or retraction into moving bases. In a following study, Lee [13] investigated a similar axially extending and rotating beam, but with the effects of gravity and setting angle. Furthermore, Tadikonda *et al.* [14] presented a model for the complete dynamics of a flexible structure during deployment from a moving base. They gave a recursive solution method for an efficient numerical simulation of the dynamics equation, in a multi-body formalism. In addition to these works related to linear beams, a very comprehensive study on the geometrically non-linear flexible sliding beams was performed by Vu-Quoc and Li [15]. They employed the so called exact beam theory presented in references [16, 17]. The beams can undergo large deformation, large overall motion, with shear deformation accounted for. Following the approach outlined by Vu-Quoc and Li, Behdinan *et al.* [18] derived the equations of motion for geometrically non-linear flexible beams, deployed and retrieved through prismatic joints. They provided an alternative formulation in which by superposition of a prescribed axial velocity the beam is brought to rest and the channel assumes the prescribed velocity. As the second part of this study, the transient response of axially inextensible sliding beams has been computed by Behdinan and Tabarrok [19]. They used Galerkin's method and presented several illustrative cases showing the differences between the linear and non-linear solutions to these problems.

Since robot manipulators are the main areas for the application of axially moving beams, Chalhoub and Ulsoy [20] investigated a robot arm which has two revolute joints and one prismatic joint. They used an assumed modes method in their simulation studies. In a different study, Wang and Wei [21] considered a robot with a long extendible robot arm which can undergo both vertical translation and rotary motion. They used Newton's second law to derive the equations of motion for the flexible arm and made use of a Galerkin type approximation to solve them. In a following study, adding the vibration of the arm's tail section, the latter has been revised by Krishnamurthy [22]. He applied Galerkin's procedure to the equations of motion derived by means of the extended Hamilton's principle. Buffinton [23] studied a Stanford-like manipulator consisting of a uniform elastic beam connected at one end to a rigid block and capable of moving longitudinally over supports attached to a rotating base. He has applied the basic techniques developed by Buffinton and Kane [5] to this specific study. By taking account of the stiffening, end-mass and gravitational effects, Al-Bedoor and Khulief [24] developed a general dynamic model for an elastic beam with prismatic and revolute joints.

To develope a general model for design and control of flexible manipulators with prismatic joints, Pan *et al.* [25] have studied a robotic manipulator model consisting of a sequence of links connected either by revolute or prismatic joints. They have also taken into account the axial shortening effect of the beam. To further validate their model and numerical procedures, they have performed experiments on a spherical co-ordinate robot with one prismatic joint and two revolute joints [26]. They reported both experimental and numerical results. Recently, Al-Bedoor and Khulief [27] developed a general dynamic model for a sliding flexible link through a prismatic joint where the prismatic joint hub is executing general planar motion. They adopted the finite element formulation with a fixed number of elements, where each element has a constant length. As a more general problem, a robot with a flexible arm having a translational motion through an arbitrarily driven prismatic joint has been investigated by Gürgöze and Müller [28]. They have used two approaches, continuum and multibody models to formulate the vibration problems of an elastic robot arm in flexure and torsion.

In almost all the studies related to linear beam theory so far, Euler–Bernoulli beam assumption, neglecting the effects of rotary inertia and shear deformation, has been used to investigate the vibrations of axially moving flexible beams. Some of them have included the axial force effect in this vibration problem, some have added structural damping effect only or both. Additionally in some studies, researchers have attached a concentrated mass to one end of the beam, in some others, they have attached an end-force and moment. Furthermore, the tail section of the moving beam has been investigated by Krishnamurthy [22].

In the present paper, a more general problem including most of the effects mentioned above is discussed. Considering the effects of the rotary inertia, axial force due to inertial forces of the motion of the prismatic joint

associated with axial foreshortening, end mass and the tail section of the beam; the flexural vibrations of a linear flexible beam moving axially through an arbitrarily driven prismatic joint are investigated. When the dynamic system is restricted to the x-y horizontal plane, the gravitational effects can be neglected. It is also assumed that the effects of shear deformation, axial deformation and structural damping are negligible.

Here, the equations of motion of the dynamic system described above are derived via extended Hamilton's principle. Due to difficulties in finding a direct analytical solution to this time dependent partial differential equation and its boundary conditions, discretization by means of a series solution, called also the assumed modes method, is developed in order to obtain an approximate solution. In the rest of the paper, some sample results for various kinematic inputs of the prismatic joint and physical values of the dynamic system are presented.

2. EQUATIONS OF MOTION

The dynamic system to be considered is shown in Figure 1. It consists of an elastic beam in flexure with a concentrated end-mass M, sliding through a prismatic joint whose kinematics is given by the angle $\gamma(t)$, and the position vector $\mathbf{r}(t)$ of its central point A. It is assumed that the elements of the system are constrained to move on the horizontal x-y plane. The beam is driven according to $u(t)$.

As is shown in Figure 1, there are three co-ordinate systems to be used in the mathematical analysis of the dynamic system. One of them is an inertial co-ordinate system denoted by XYZ and, the other two are moving co-

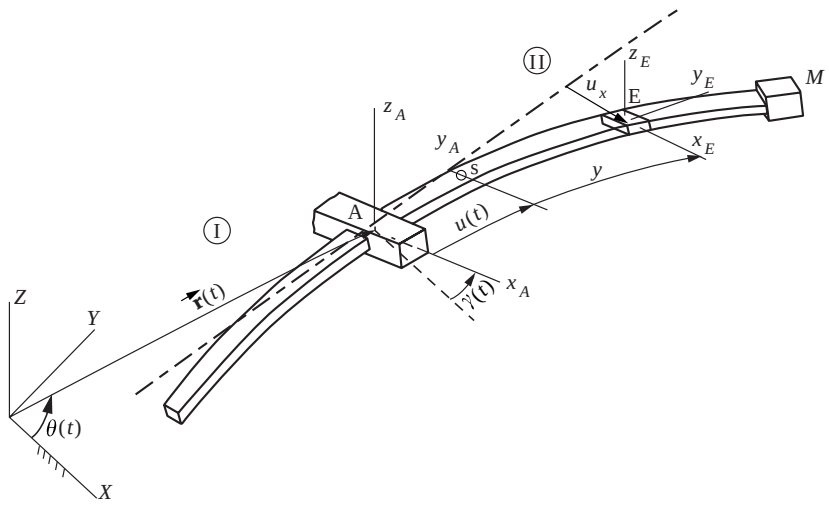

Figure 1. A flexible beam sliding through a prismatic joint.

ordinate systems denoted by $x_A y_A z_A$ attached at point A to the prismatic joint, and $x_E y_E z_E$ attached to a typical element at point E on the elastic beam.

The equations of motion will be derived by applying the extended Hamilton's principle

$$\int_{t_1}^{t_2} [\delta(T - V) + \delta' A] \, \mathrm{d}t = 0, \tag{1}$$

where T denotes, as usual, the kinetic energy, V denotes the potential energy and $\delta' A$ represents the virtual work done by non-conservative forces acting on the system. Here, however, the virtual work of the driving force is zero ($\delta' A = 0$) since the sliding motion $u(t)$ is a prescribed motion and therefore its variation is zero ($\delta u = 0$).

The kinetic energy consists of two parts which are due to translation and rotation of each element of the beam. Dividing the beam into two parts as the front and the tail sections, the rotational kinetic energy is

$$T_{rot} = \frac{\rho I_z}{2} \int_{-L/2}^{-u} (\dot{\gamma} - \dot{u}'_{x_1})^2 \, \mathrm{d}y + \frac{\rho I_z}{2} \int_{-u}^{L/2} (\dot{\gamma} - \dot{u}'_{x_2})^2 \, \mathrm{d}y. \tag{2}$$

Here, ρ shows mass density, I_z shows the moment of inertia with respect to axis z_E for the uniform beam cross-section, $u_{x_1}(y, t)$ and $u_{x_2}(y, t)$ present the bending displacement corresponding to the two sections of the beam and γ denotes the rotation angle of the prismatic joint about z_A-axis. Primes and dots in the above equation refer to partial derivatives with respect to the position co-ordinate y and time t respectively.

In a similar fashion, by utilizing the absolute translational velocity vector with respect to $x_A y_A z_A$ co-ordinate system, of a typical element at point E on the elastic beam, in the form

$$\mathbf{V}_{E_A} = \begin{Bmatrix} \nu_{A_x} \cos\gamma + \nu_{A_y} \sin\gamma + \dot{u}_x - \dot{\gamma}(u + y) \\ -\nu_{a_x} \sin\gamma + \nu_{A_y} \cos\gamma + \dot{u} + \dot{\gamma} u x \\ 0 \end{Bmatrix} \tag{3}$$

then, the translational kinetic energy can be obtained as

$$\begin{aligned} T_{trans} = \frac{1}{2} \int_{-L/2}^{-u} \rho A [& \nu_{A_x}^2 + \nu_{A_y}^2 + \dot{u}_{x_1}^2 + \dot{\gamma}^2 (u + y)^2 - 2\dot{u}_{x_1} \dot{\gamma}(u + y) + \dot{u}^2 + \dot{\gamma}^2 u_{x_1}^2 \\ & + 2\dot{u}\dot{\gamma} u_{x_1} + 2\{\dot{u}_{x_1} - \dot{\gamma}(u + y)\}(\nu_{A_x} \cos\gamma + \nu_{A_y} \sin\gamma) - 2(\dot{\gamma} u_{x_1} + \dot{u}) \\ & \times (\nu A_x \sin\gamma - \nu A_y \cos\gamma)] \, \mathrm{d}y + \frac{1}{2} \int_{-u}^{L/2} \left[\rho A + M\delta\left(y - \frac{L}{2}\right) \right] [\nu_{A_x}^2 + \nu_{A_y}^2 + \dot{u}_{x_2}^2 \\ & + \dot{\gamma}^2 (u + y)^2 - 2\dot{u}_{x_2} \dot{\gamma}(u + y) + \dot{u}^2 + \dot{\gamma}^2 u_{x_2}^2 + 2\dot{u}\dot{\gamma} u_{x_2} + 2\{\dot{u}_{x_2} - \dot{\gamma}(u + y)\} \\ & \times (\nu_{A_x} \cos\gamma + \nu_{A_y} \sin\gamma) - 2(\dot{\gamma} u_{x_2} + \dot{u})(\nu_{A_x} \sin\gamma - \nu_{A_y} \cos\gamma)] \, \mathrm{d}y, \end{aligned} \tag{4}$$

where A is the cross-sectional area of the beam, M is the concentrated end mass, and ν_{A_x} and ν_{A_y} are the x and y components of translational velocity of the central point A of the prismatic joint, expressed in the inertial co-ordinate system. In equation (4), a spatial Dirac delta function is defined as

$$\delta\left(y-\frac{L}{2}\right)=0, \quad y\neq\frac{L}{2}$$

$$\int_{-u}^{L/2}\delta\left(y-\frac{L}{2}\right)\,\mathrm{d}y=1. \tag{5}$$

On the other hand, the potential energy also consists of two parts. One of them is the strain energy due to the bending and the other is the potential energy associated with the axial force arising due to inertial forces in connection with the so called axial foreshortening.

Let the potential energy due to the bending be written in the form

$$V_{e_1}=\tfrac{1}{2}\int_{-L/2}^{-u}EI_z u_{x_1}^{''2}\,\mathrm{d}y+\tfrac{1}{2}\int_{-u}^{L/2}EI_z u_{x_2}^{''2}\,\mathrm{d}y \tag{6}$$

as the beam has two parts. Here, EI_z denotes flexural rigidity.

Furthermore, the potential energy coming from the axial force associated with foreshortening can be written as

$$V_{e_2}=\tfrac{1}{2}\int_{-L/2}^{-u}P_1(y,\,t)u_{x_1}^{'2}\,\mathrm{d}y+\tfrac{1}{2}\int_{-u}^{L/2}P_2(y,\,t)u_{x_2}^{'2}\,\mathrm{d}y, \tag{7}$$

where $P_1(y,\ t)$ and $P_2(y,\ t)$ are the axial forces. Differentiating the second element of the velocity vector in equation (3), the absolute acceleration of a typical element at point E on the elastic beam with respect to the axis y_A is

$$\alpha_{E_y}=\ddot{u}-\dot{\nu}_{A_x}\sin\gamma+\dot{\nu}_{A_y}\cos\gamma-\dot{\gamma}^2(u+y). \tag{8}$$

From this equation, two different expressions for the axial forces can be written as; for the tail section

$$P_1(y,\,t)=\rho A[(\ddot{u}-\dot{\gamma}^2u+\dot{\nu}_{A_y}\cos\gamma-\dot{\nu}_{A_x}\sin\gamma)(y+L/2)+(\dot{\gamma}^2/2)(L^2/4-y^2)], \tag{9}$$

and for the front section

$$P_2(y,\,t)=-M[\ddot{u}-\dot{\gamma}^2(u+L/2)+\dot{\nu}_{A_y}\cos\gamma-\dot{\nu}_{A_x}\sin\gamma]$$

$$+\rho A[(\ddot{u}-\dot{\gamma}^2u+\dot{\nu}_{A_y}\cos\gamma-\dot{\nu}_{A_x}\sin\gamma)(y-L/2)+(\dot{\gamma}^2/2)(L^2/4-y^2)] \tag{10}$$

As stated before, $u(t)$ denotes the sliding motion of the rigid beam with

respect to the prismatic joint. The terms associated with the elastic displacement are neglected in equations (8) to (10)

At this point, summing the kinetic and potential energy terms as

$$T = T_{rot} + T_{trans}, \qquad V = V_{e_1} + V_{e_2} \tag{11}$$

and then, making use of Hamilton's principle given in (1), one can obtain the equations of motion for the tail section ($-L/_2 < y < -u$) in the following form

$$\begin{aligned}
&[-\ddot{u}_{x_1} + 2\dot{\gamma}\dot{u} + \ddot{\gamma}(u+y) + \dot{\gamma}^2 u_{x_1} - \dot{\nu}_{A_x}\cos\gamma - \dot{\nu}_{A_y}\sin\gamma] \\
&\quad + [(\ddot{u} - \dot{\gamma}^2 u + \dot{\nu}_{A_y}\cos\gamma - \dot{\nu}_{A_x}\sin\gamma)(y + L/2) + (\dot{\gamma}^2/2)(L^2/4 - y^2)]u''_{x_1} \\
&\quad + [\ddot{u} - \dot{\gamma}^2(u+y) + \dot{\nu}_{A_y}\cos\gamma - \dot{\nu}_{A_x}\sin\gamma]u'_{x_1} + (I_z/A)\ddot{u}''_{x_1} - (EI_z/\rho A)u^{iv}_{x_1} = 0,
\end{aligned} \tag{12}$$

and for the front section ($-u < y < L/2$) as

$$\begin{aligned}
&[1 + (M/\rho A)\delta(y - L/2)][-\ddot{u}_{x_2} + 2\dot{\gamma}\dot{u} + \ddot{\gamma}(u+y) + \dot{\gamma}^2 u_{x_2} - \dot{\nu}_{A_x}\cos\gamma - \dot{\nu}_{A_y}\sin\gamma] \\
&\quad + [(\ddot{u} - \dot{\gamma}^2 u + \dot{\nu}_{A_y}\cos\gamma - \dot{\nu}_{a_X}\sin\gamma)(y - L/2) + (\dot{\gamma}^2/2)(L^2/4 - y^2) \\
&\quad - (M/\rho A)\{\ddot{u} - \dot{\gamma}^2(u + L/2) + \dot{\nu}_{A_y}\cos\gamma - \dot{\nu}_{A_x}\sin\gamma\}]u''_{x_2} + [\ddot{u} - \dot{\gamma}^2(u+y) \\
&\quad + \dot{\nu}_{A_y}\cos\gamma - \dot{\nu}_{A_x}\sin\gamma]u'_{x_2} + (I_z/A)\ddot{u}''_{x_2} - (EI_z/\rho A)u^{iv}_{x_2} = 0
\end{aligned} \tag{13}$$

In addition to the differential equations of motion that must be satisfied over the length of the beam, a few associated boundary condition terms also remain to be satisfied. These are,

$$\begin{aligned}
&u_{x_1}(-u, t) = u_{x_2}(-u, t) = 0, \qquad u'_{x_1}(-u, t) = u'_{x_2}(-u, t) = 0, \\
&u''_{x_1}(-L/2, t) = u''_{x_2}(L/2, t) = 0, \quad [\rho I_z(\ddot{\gamma} - \ddot{u}'_{x_1}) + EI_z u'''_{x_1}]|_{y=-L/2} = 0, \\
&[\rho I_z(\ddot{\gamma} - \ddot{u}'_{x_2}) + EI_z u'''_{x_2} + M\{\ddot{u} - \dot{\gamma}^2(u + L/2) + \dot{\nu}_{A_y}\cos\gamma - \dot{\nu}_{A_x}\sin\gamma\}]|_{y=L/2} = 0.
\end{aligned} \tag{14}$$

Here, the last two boundary conditions result from utilizing Hamilton's principle. These equations of motion and associated eight boundary conditions describe a complex boundary value problem for which an exact solution is not possible. Therefore, approximate methods are to be used to solve this type of boundary value problems.

3. APPROXIMATE SOLUTION

Since an exact solution is not possible due to the complexity of the differential equations themselves and the associated boundary conditions, the partial differential equations of motion of the dynamic system will be discretized by

means of the assumed modes method in order to obtain an approximate solution. For the transverse vibrations $u_{x_1}(y, t)$ and $u_{x_2}(y, t)$, the method consists of assuming solutions in the form of infinite series as

$$u_{x_1} = \sum_{j=1}^{\infty} e_{j1}(y, t) q_{j1}(t), \qquad u_{x_2} = \sum_{j=1}^{\infty} e_{j2}(y, t) q_{j2}(t), \tag{15}$$

where $e_{j1}(y, t)$ and $e_{j2}(y, t)$ are properly selected admissible functions that depend on the spatial co-ordinate y and time t, and $q_{j1}(t)$ and $q_{j2}(t)$ are the time-dependent generalized co-ordinates to be determined. Here, the eigenfunctions of a clamped–free beam are chosen as the functions $e_{j1}(y, t)$ and $e_{j2}(y, t)$ since they satisfy all of the geometric boundary conditions of the system. They are

$$\begin{aligned} e_{j1}(y, t) = {} & \cosh\left(\hat{\lambda}_j \frac{u+y}{u-L/2}\right) - \cos\left(\hat{\lambda}_j \frac{u+y}{u-L/2}\right) - \eta_j \left[\sinh\left(\hat{\lambda}_j \frac{u+y}{u-L/2}\right)\right. \\ & \left. - \sin\left(\hat{\lambda}_j \frac{u+y}{u-L/2}\right)\right], \quad e_{j2}(y, t) = \cosh\left(\hat{\lambda}_j \frac{u+y}{u+L/2}\right) - \cos\left(\hat{\lambda}_j \frac{u+y}{u+L/2}\right) \\ & - \eta_j \left[\sinh\left(\hat{\lambda}_j \frac{u+y}{u+L/2}\right) - \sin\left(\hat{\lambda}_j \frac{u+y}{u+L/2}\right)\right], \end{aligned} \tag{16}$$

where

$$\eta_j = (\cos \hat{\lambda}_j + \cos \hat{\lambda}_j)/(\sinh \hat{\lambda}_j + \sin \hat{\lambda}_j) \tag{17}$$

and the dimensionless frequency parameters $\hat{\lambda}_j$ satisfy the characteristic equation of a clamped–free beam

$$\cosh \hat{\lambda}_j \cos \hat{\lambda}_j = -1, \quad j = 1, \cdots, \infty \tag{18}$$

Furthermore, it can be shown that these eigenfunctions satisfy the following conditions at the boundaries:

$$\begin{aligned} & e_{j1}(-u, t) = e'_{j1}(-u, t) = e''_{j1}(-L/2, t) = e'''_{j1}(-L/2, t) = 0, \\ & e_{j2}(-u, t) = e'_{j2}(-u, t) = e''_{j2}(L/2, t) = e'''_{j2}(L/2, t) = 0 \end{aligned} \tag{19}$$

It is seen that $u_{x_1}(y, t)$ and $u_{x_2}(y, t)$ given in (14) satisfy all of the geometric boundary conditions and additionally also two of the dynamic (natural) boundary conditions in (14). Therefore, they can be used as admissible functions for this boundary value problem according to the assumed modes method [29].

Now, substituting the infinite series given by (15) into the kinetic and potential energy terms given by (2), (4) and (6), (7)–(11), then using them in Lagrange's

equations

$$\mathrm{d}/\mathrm{d}t(\partial T/\partial \dot{q}_{ji}) - \partial T/\partial q_{ji} + \partial V/\partial q_{ji} = 0; \quad i = 1, 2, \quad j = 1, \cdots, \infty, \tag{20}$$

one can obtain the equations of motion as an infinite system of ordinary differential equations with time varying coefficients. Introducing the definitions

$$u_1 = \frac{u}{u - L/2}, \quad u_2 = \frac{1}{u - L/2}, \quad u_3 = \frac{u}{u + L/2}, \quad u_4 = \frac{1}{u + L/2} \tag{21}$$

and making use of the conditions given in (19), and using the orthogonality property of the eigenfunctions, the equations of motion for the tail and front sections of the beam can be written after considerably lengthy calculations as

$$\begin{aligned}
\sum_{j=1}^{\infty} \Bigg\{ & \left[\delta_{jk} \left(\frac{L}{2} - u \right) + \frac{I_z}{A} \int_{-L/2}^{-u} e_{j1}' e_{k1}' \, \mathrm{d}y \right] \ddot{q}_{j1} \\
& + \left[2 \int_{-L/2}^{-u} \left(\frac{\dot{u}_1 + \dot{u}_2 y}{u_2} e_{j1}' e_{k1} + \frac{I_z}{A} \frac{\dot{u}_2}{u_2} e_{j1}' e_{k1}' + \frac{I_z}{A} \frac{\dot{u}_1 + \dot{u}_2 y}{u_2} e_{j1}'' e_{k1}' \right) \mathrm{d}y \right] \dot{q}_{j1} \\
& + \Bigg[\delta_{jk} \left(\frac{L}{2} - u \right) \left(\frac{EI_z}{\rho A} \hat{\lambda}_k^4 u_2^4 - \dot{\gamma}^2 \right) + \int_{-L/2}^{-u} \Bigg\langle \frac{\ddot{u}_1 + \ddot{u}_2 y}{u_2} e_{j1}' e_{k1} \\
& + \left\{ (\ddot{u} - \dot{\gamma}^2 u - \dot{\nu}_{A_x} \sin\gamma + \dot{\nu}_{A_y} \cos\gamma) \left(y + \frac{L}{2} \right) - \frac{\dot{\gamma}^2}{2} \left(y^2 - \frac{L^2}{4} \right) + \frac{I_z}{A} \frac{\ddot{u}_2}{u_2} \right\} e_{j1}' e_{k1}' \\
& + \frac{(\dot{u}_1 + \dot{u}_2 y)^2}{u_2^2} e_{j1}'' e_{k1}' + \frac{I_z}{A} \frac{2\dot{u}_2(\dot{u}_1 + \dot{u}_2 y) + u_2(\ddot{u}_1 + \ddot{u}_2 y)}{u_2^2} e_{j1}'' e_{k1}' \\
& + \frac{I_z}{A} \frac{(\dot{u}_1 + \dot{u}_2 y)}{u_2^2} e_{j1}''' e_{k1}' \Bigg\rangle \, \mathrm{d}y \Bigg] q_{j1} - \int_{-L/2}^{-u} \Bigg\langle \ddot{\gamma} \left\{ \frac{I_z}{A} e_{k1}' + (u + y) e_{k1} \right\} \\
& + (2\dot{u}\dot{\gamma} - \dot{\nu}_{A_x} \cos\gamma - \dot{\nu}_{A_y} \sin\gamma) e_{k1} \Bigg\rangle \, \mathrm{d}y \Bigg] \Bigg\} = 0, \quad k = 1, \cdots, \infty,
\end{aligned} \tag{22}$$

and

$$\sum_{j=1}^{\infty}\Bigg\{\Bigg[\int_{-u}^{L/2}\left\langle\left(1+\frac{M}{\rho A}\delta\left(y-\frac{L}{2}\right)\right)e_{j2}e_{k2}+\frac{I_z}{A}e_{j2}'e_{k2}'\right\rangle\,\mathrm{d}y\Bigg]\ddot{q}_{j2}$$

$$+\Bigg[2\int_{-u}^{L/2}\left\langle\left(1+\frac{M}{\rho A}\delta\left(y-\frac{L}{2}\right)\right)\frac{\dot{u}_3+\dot{u}_4 y}{u_4}e_{j2}'e_{k2}$$

$$+\frac{I_z}{A}\left(\frac{\dot{u}_4}{u_4}e_{j2}'e_{k2}'+\frac{\dot{u}_3+\dot{u}_4 y}{u_4}e_{j2}''e_{k2}'\right)\right\rangle\,\mathrm{d}y\Bigg]\dot{q}_{j2}$$

$$+\Bigg[\int_{-u}^{L/2}\left\langle\left(1+\frac{M}{\rho A}\delta\left(y-\frac{L}{2}\right)\right)\left(\frac{\ddot{u}_3+\ddot{u}_4 y}{u_4}e_{j2}'e_{k2}+\frac{(\dot{u}_3+\dot{u}_4 y)^2}{u_2^2}e_{j2}''e_{k2}-\dot{\gamma}^2 e_{j2}e_{k2}\right)\right.$$

$$+\frac{I_z}{A}\left(\frac{\ddot{u}_4}{u_4}e_{j2}'e_{k2}'+\frac{2\dot{u}_4(\dot{u}_3+\dot{u}_4 y)+u_4(\ddot{u}_3+\ddot{u}_4 y)}{u_4^2}e_{j2}''e_{k2}'+\frac{(\dot{u}_3+\dot{u}_4 y)^2}{u_2^2}e_{j2}'''e_{k2}'\right)$$

$$+\left(\frac{EI_z}{\rho A}e_{j2}''e_{k2}''\right)+\Bigg(-\frac{M}{\rho A}\{\ddot{u}-\dot{\gamma}^2(u+y)-\dot{\nu}_{A_x}\sin\gamma+\dot{\nu}_{A_y}\cos\gamma\}$$

$$\left.+(\ddot{u}-\dot{\gamma}^2 u-\dot{\nu}_{A_x}\sin\gamma+\dot{\nu}_{A_y}\cos\gamma)\left(y-\frac{L}{2}\right)-\frac{\dot{\gamma}^2}{2}\left(y^2-\frac{L^2}{4}\right)\right)e_{j2}'e_{k2}'\right\rangle\,\mathrm{d}y\Bigg]q_{j2}$$

$$-\Bigg[\int_{-u}^{L/2}\left\langle\left(1+\frac{M}{\rho A}\delta\left(y-\frac{L}{2}\right)\right)\{\ddot{\gamma}(u+y)+2\dot{u}\dot{\gamma}-\dot{\nu}_{A_x}\cos\gamma-\dot{\nu}_{A_y}\sin\gamma\}e_{k2}\right.$$

$$\left.+\frac{I_z}{A}\ddot{\gamma}e_{k2}'\right\rangle\,\mathrm{d}y\Bigg]\Bigg\}=0,\qquad k=1,\cdots,\infty, \tag{23}$$

where δ_{jk} denotes the Kronecker delta. These equations completely represent the dynamics of the system and will be used for simulation studies.

For the sake of completeness, another set of ordinary differential equations with time varying coefficients is obtained by introducing the infinite series given in (15) directly into the extended Hamilton's principle given in equation (1) together with equations (2)–(11), but not presented here. Those equations are apparently different from the equations given by equations (22) and (23) but one can verify easily that they are equal after doing some simple mathematical rearrangements.

4. NUMERICAL RESULTS

The approximate equations of motion of the dynamic system can be solved by using one of the common Runge–Kutta computational algorithms. Taking finite series instead of infinite ones given in (15), simulation studies are performed for

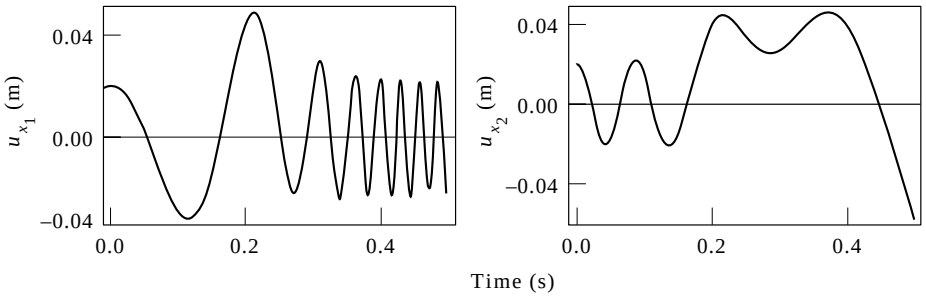

Figure 2. Tip deflections for $r = 1$ m, $u_0 = -0{\cdot}35$ m, $u_t = 0{\cdot}7$ m, $\theta_t = \gamma_t = \pi$ rad, $T = 0{\cdot}5$ s, $M = 0{\cdot}15$ kg.

typical cases. Due to its importance in the applications of the axially moving beam, the tip deflections of the tail and front sections of the beam are calculated in the simulation studies by taking 1–3 terms. Since there is not much difference among the results, the illustrations of the tip deflections are presented by using the two terms of the series in the following figures. In numerical examples, it is assumed that the beam material is aluminum for which the density is $\rho = 2700$ kg/m^3 and the modulus of elasticity is $E = 7 \times 10^{10}$ N/m^2. For the beam geometry, the following values are used; the cross-sectional area $A = 0{\cdot}000075$ m^2, the moment of inertia $I_z = 1{\cdot}563 \times 10^{-10}$ m^4, and the length of the beam $L = 1{\cdot}4$ m, which makes the beam very slender. Different end-masses ($M = 0{\cdot}15$ kg and $M = 0{\cdot}30$ kg) are also used in order to investigate end-mass effects on the vibrations.

In simulation studies, similar to those of references [5, 11] for comparison, the following functions are used to generate the translational and rotational motions;

$$\begin{aligned} u(t) &= u_0 + (u_t/T)[t - (T/2\pi)\sin(2\pi t/T)], \\ \gamma(t) &= \gamma_0 + (\gamma_t/T)[t - (T/2\pi)\sin(2\pi t/T)], \\ \theta(t) &= \theta_0 + (\theta_t/T)[t - (T/2\pi)\sin(2\pi t/T)], \end{aligned} \tag{24}$$

where u_0, θ_0 and γ_0 denote the initial length and angles; u_t, θ_t and γ_t denote the total displacement and angles respectively (Figure 1), and T denotes the operating period.

Figure 2, as a typical case, represents the tip deflections of the beam whose front section (II) has an extending motion through the prismatic joint. The central point of the joint is moving on a circle around the axis Z, where the radius r of the circle is constant. Since the input parameters given in the legend represent a high speed operation of the beam, the tip deflections are large as expected. In the figure, the tip deflection of the front section increases when its length increases; in a similar manner, the tip deflection of the tail section decreases when its length decreases. This makes clear that decreasing length gives rise to the stiffness of the beam. Figures 3–7 are plotted using the same input

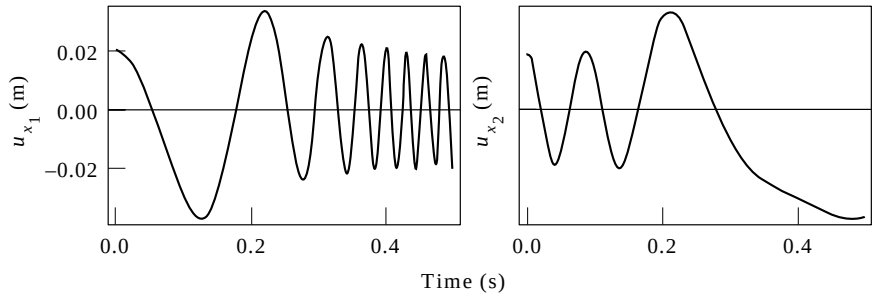

Figure 3. Tip deflections for $r = 0$, $u_0 = -0{\cdot}35$ m, $u_t = 0{\cdot}7$ m, $\gamma_t = \pi$ rad, $T = 0{\cdot}5$ s, $M = 0{\cdot}15$ kg.

parameters as those of Figure 2 except one in every figure, so that its effect can be seen in comparison with Figure 2.

Figure 3 illustrates the tip deflections of another typical case of the sliding beam. In this case, the central point A of the prismatic joint coincides with the center of the inertial coordinate system ($r = 0$), and the joint has a rotational motion around the axis Z while the beam has an axial motion through it. By comparing Figure 3 with Figure 2, it is seen that such a rotation leads to smaller tip deflections for both front and tail sections.

Figure 4 represents the tip deflections for the case when the beam front section retracts into the prismatic joint. All inputs of Figure 4 are the same as those of Figure 2 with the exception that the motion of the front section is a retraction not a deployment. As expected, the deflection of the front section decreases and the deflections of the tail section increases as the beam slides.

As it can be seen from Figure 5 the larger end mass results in the larger tip deflections. The end mass in Figure 5 is double that in Figure 2. There is a sharp increase in the tip deflection of the beam front section, showing that an extending beam with a larger end mass has higher amplitudes.

To illustrate the effect of the beam orientation as the joint rotates, Figure 6 is plotted for $\theta(t) = \gamma(t) - \pi/2$. This means that the position vector $\mathbf{r}(t)$ is rotating by an angle $\theta(t)$ about the axis Z while the prismatic joint is rotating by an angle $\gamma(t)$ about axis z_A; then, the mode shapes of the tip deflections are different from those of Figure 2. In a similar manner, Figure 7 presents the tip deflections in

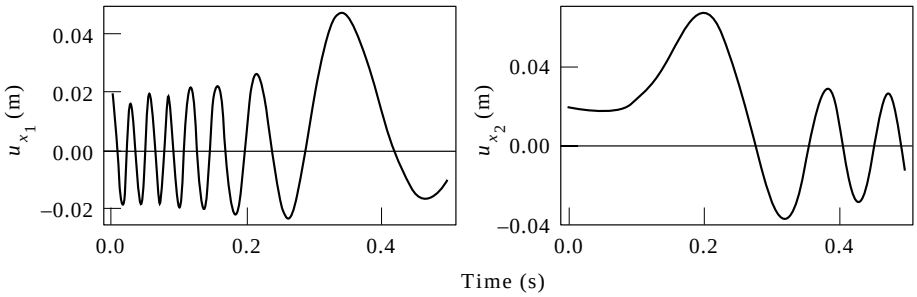

Figure 4. Tip deflections for $r = 1$ m, $u_0 = 0{\cdot}35$ m, $u_t = -0{\cdot}7$ m, $\theta_t = \gamma_t = \pi$ rad, $T = 0{\cdot}5$ s, $M = 0{\cdot}15$ kg.

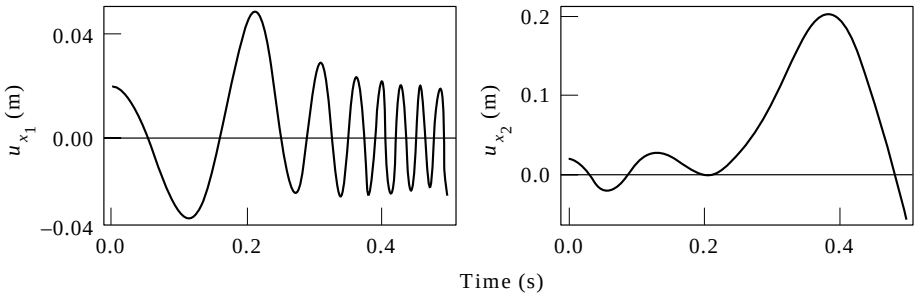

Figure 5. Tip deflections for $r = 1$ m, $u_0 = -0{\cdot}35$ m, $u_t = 0{\cdot}7$ m, $\theta_t = \gamma_t = \pi$ rad, $T = 0{\cdot}5$ s, $M = 0{\cdot}30$ kg.

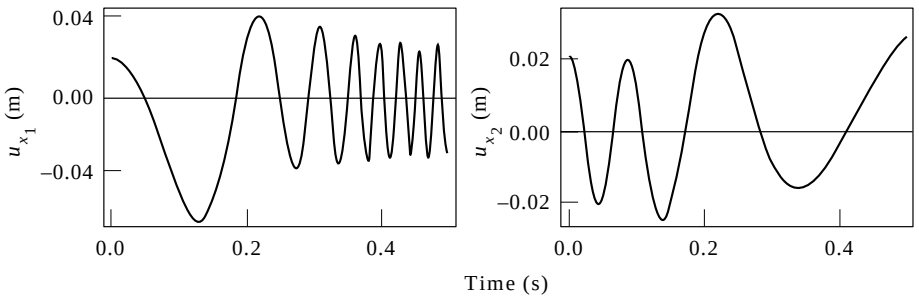

Figure 6. Tip deflections for $r = 1$ m, $u_0 = -0{\cdot}35$ m, $u_t = 0{\cdot}7$ m, $\gamma_t = \pi$ rad, $\theta_t = \gamma_t - \pi/2$ rad, $T = 0{\cdot}5$ s, $M = 0{\cdot}15$ kg.

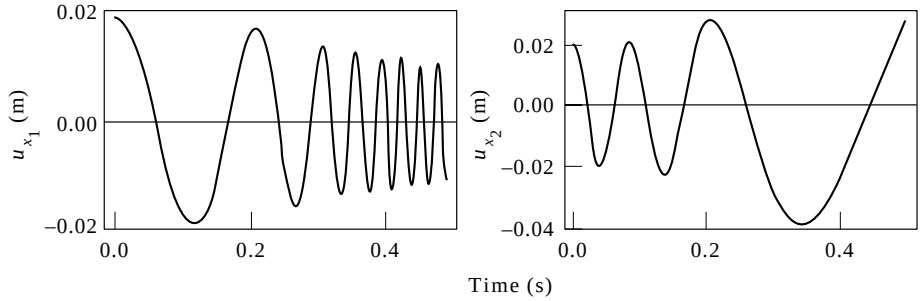

Figure 7. Tip deflections for $r = 1$ m, $u_0 = -0{\cdot}35$ m, $u_t = 0{\cdot}7$ m, $\theta_t = \pi$ rad, $\gamma_t = 0$, $T = 0{\cdot}5$ s, $M = 0{\cdot}15$ kg.

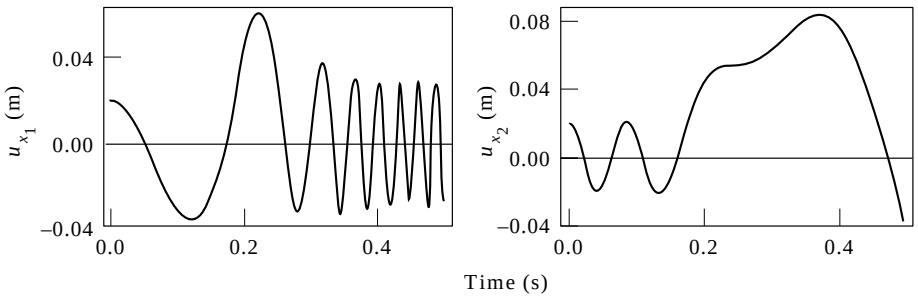

Figure 8. Tip deflections for $r = 1$ m, $u_0 = -0{\cdot}35$ m, $u_t = 0{\cdot}7$ m, $\theta_t = \gamma_t = \pi$ rad, $T = 0{\cdot}5$ s, $M = 0{\cdot}15$ kg and no axial force.

which the prismatic joint does not rotate ($\gamma = 0$). This leads to smaller tip deflections in comparison with the tip deflections in Figures 2 and 6.

To see the effect of the axial force due to inertial forces associated with the axial foreshortening, Figure 8 is plotted without axial force effect. Comparison between the results of Figure 2 and Figure 8 shows that neglecting the axial force leads to larger tip deflections. Although the tip deflections increase in this example, increase or decrease in the deflection depends on the orientation of the axial force given in (9) and (10). Furthermore, it can be seen from other numerical studies not mentioned here that the axial force effect in low speed operations can be neglected since the results with and without the axial force effect are identical.

Table 1 represents the tip deflections with and without the rotary inertia effect. It can be seen from the table that the results with and without the rotary inertia effect are slightly different, and so the differences cannot be shown in graphical form. Thus, the rotary inertia effect can be neglected even if the beam is moving at high speeds. However, one can take the rotary inertia effect into consideration in a special case like a sensitive operation.

5. CONCLUSIONS

The flexural vibrations of a flexible linear beam moving axially through an arbitrarily driven prismatic joint on a horizontal plane are investigated. The

TABLE 1

Tip deflection with and without rotary inertia effect for $r = 1$ m, $u_0 = -0{\cdot}35$ m, $u_t = 0{\cdot}7$ m, $\theta_t = \gamma_t = \pi$ rad, $T = 0{\cdot}5$ s, $M = 0{\cdot}15$ kg.

Time (s)	u_{x_1}(m), with rotary inertia	$u_{x_1}(m)$ without rotary inertia	u_{x_2} (m), with rotary inertia	$u_{x_2}(m)$, without rotary inertia
0·1	−0·0291229	−0·0291231	0·0147087	0·0147082
0·2	0·0462643	0·0462646	0·0399119	0·0399123
0·3	0·0225237	0·0225256	0·0269203	0·0269192
0·4	0·0232226	0·0232217	0·0394299	0·0394311
0·5	−0·0219838	−0·0219814	−0·0576182	−0·0576176

effects of rotary inertia, axial force associated with axial shortening and end mass are considered together with the Euler–Bernoulli beam assumption. The vibrations of the beam tail section are also included in the problem. The equations of motion and the associated boundary conditions are derived by using the extended Hamilton's principle. Since they form a very complex boundary value problem for which an exact solution is not possible, the assumed modes method is used to obtain an approximate solution. These equations are solved to simulate the system for some typical joint kinematics. The corresponding numerical results are given in the forms of plots and a table. The results show that the axial force effect must be considered in high speed operations, whereas the rotary inertia effect can be neglected even in high speed operations.

REFERENCES

1. B. Tabarrok, C. M. Scott and Y. L. Kim 1997 *Journal of Franklin Institute* **297**, 201–220. On the dynamics of an axially moving beam.
2. S. Bergamaschi and A. Sinopoli 1983 *Mechanical Research Communications* **10**, 341–345. On the flexural vibrations of arms with variable length: an exact solution.
3. P. K. C. Wang and J. D. Wei 1987 *Journal of Sound and Vibration* **114**, 149–160. Vibrations in a moving flexible robot arm.
4. S. S. K. Tadikonda and H. Baruh 1992 *Journal of Dynamic Systems, Measurements and Control* **114**, 422–427. Dynamics and control of a translating flexible beam with a prismatic joint.
5. K. W. Buffinton and T. R. Kane 1985 *International Journal of Solids Structure* **21**, 617–643. Dynamics of a beam over supports.
6. H. P. Lee 1993 *International Journal of Solids Structure* **30**, 199–209. Dynamics of a beam over multiple supports.
7. M. Stylianou and B. Tabarrok 1993 *Journal of Sound and Vibration* **178**, 433–453. Finite element analysis of an axially moving beam, part I: time integration.
8. M. Stylianou and B. Tabarrok 1993 *Journal of Sound and Vibration* **178**, 455–481. Finite element analysis of an axially moving beam, part II: stability analysis.
9. R. J. Theodore, J. H. Arakeri and A. Ghosal 1996 *Journal of Sound and Vibration* **191**, 363–376. The modelling of axially translating flexible beams.
10. B. O. Al-Bedoor and Y. A. Khulief 1996 *Journal of Sound and Vibration* **192**, 159–171. An approximate analytical solution of beam vibrations during axial motion.
11. J. Yuh and T. Young 1991 *Journal of Dynamic Systems, Measurements and Control* **113**, 34–40. Dynamic modeling of an axially moving beam in rotation: simulation and experiment.
12. A. K. Banerjee and T. R. Kane 1989 *Journal of Guidance* **12**, 140–146. Extrusion of a beam from rotating base.
13. H. P. Lee 1995 *International Journal of Solids Structures* **32**, 1595–1606. Dynamics of an axially extending and rotating cantilever beam including the effect of gravity.
14. S. S. K. Tadikonda, R. P. Singh and S. Stornelli 1996 *Journal of Vibration and Acoustics* **118**, 237–241. Multibody dynamics incorporating deployment of flexible structures.
15. L. Vu-Quoc and S. Li 1995 *Computer Methods in Applied Mechanics and Engineering* **120**, 65-118. Dynamics of sliding geometrically-exact beams: large angle maneuver and parametric resonance.
16. J. C. Simo and L. Vu-Quoc 1986 *Journal of Applied Mechanics* **53**, 849–854. On the dynamics of flexible beams under large overall motions—the plane case: part I.

17. J. C. SIMO and L. VU-QUOC 1986 *Journal of Applied Mechanics* **53**, 855–863. On the dynamics of flexible beams under large overall motions—the plane case: part II.
18. K. BEHDINAN, M. C. STYLIANOU and B. TABARROK 1997 *Journal of Sound and Vibration* **208**, 517–539. Dynamics of flexible sliding beams, non-linear analysis, part I: formulation.
19. K. BEHDINAN and B. TABARROK 1997 *Journal of Sound and Vibration* **208**, 541–565. Dynamics of flexible sliding beams, non-linear analysis, part II: transient response.
20. N. G. CHALHOUB and A. G. ULSOY 1986 *Journal of Dynamic Systems, Measurements and Control* **108**, 119–126. Dynamic simulation of a leadscrew driven flexible robot arm and controller.
21. P. K. C. WANG and J. D. WEI 1987 *IEEE International Conference on Robotics and Automation*, 1683–1689. Feedback control of vibrations in a moving flexible robot arm with rotary and prismatic joints.
22. K. KRISHNAMURTHY 1989 *Journal of Sound and Vibration* **132**, 143–154. Dynamic modeling of a flexible cylindrical manipulator.
23. K. W. BUFFINTON 1992 *Journal of Dynamic Systems, Measurements and Control* **114**, 41–49. Dynamics of elastic manipulators with prismatic joints.
24. B. O. AL-BEDOOR and Y. A. KHULIEF 1996 *Journal of Sound and Vibration* **190**, 195–206. Vibrational motion of an elastic beam with prismatic and revolute joints.
25. Y. C. PAN, R. A. SCOTT and A. G. ULSOY 1990 *Journal of Mechanical Design* **112**, 307–314. Dynamic modeling and simulation of flexible robots with prismatic joints.
26. Y. C. PAN, A. G. ULSOY and R. A. SCOTT 1990 *Journal of Mechanical Design* **112**, 315–323. Experimental model validation for a flexible robot with a prismatic joint.
27. B. O. AL-BEDOOR and Y. A. KHULIEF 1997 *Journal of Sound and Vibration* **206**, 641–661. General planar dynamics of a sliding flexible link.
28. M. GÜRGÖZE and P. C. MÜLLER 1989 *IUTAM-IFAC Symposium on Dynamics of Controlled Mechanical Systems, Switzerland*, 235–245. Modeling and control of elastic robot arm with prismatic joint.
29. L. MEIROVITCH 1967 *Analytical Methods in Vibrations*. New York: Macmillan.